Insulating states of LiBeH$_3$ under extreme compression

Chao-Hao Hu,[1,][*] Artem R. Oganov,[2,3] Andriy O. Lyakhov,[2] Huai-Ying Zhou,[1] and J. Hafner[4]

[1]*Department of Information Materials and Engineering, Guilin University of Electronic Technology,
Guangxi 541004, People's Republic of China*

[2]*Department of Geosciences and New York Center for Computational Science, Stony Brook University,
Stony Brook, New York 11794, USA*

[3]*Department of Geology, Moscow State University, 119992 Moscow, Russia*

[4]*Fakultät für Physik and Center for Computational Materials Science, Universität Wien, Sensengasse 8/12, A-1090 Wien, Austria*

High-pressure behavior of LiBeH$_3$ is investigated through *ab initio* total-energy calculations and evolutionary structure prediction simulations. Static enthalpy calculations indicate that the low-pressure phases of LiBeH$_3$ containing BeH$_4$ tetrahedra transform into the GdFeO$_3$-type perovskite *Pnma* phase at 17 GPa and then at 140 GPa into the CaIrO$_3$-type postperovskite *Cmcm* phase, both of which contain BeH$_6$ octahedra. LiBeH$_3$ remains an insulator through all these transitions and up to the pressure of 530 GPa, above which it dissociates into LiH (space group *Cmmm*) and BeH$_2$ (space group *P*4/*nmm*). Our results show that LiBeH$_3$ remains insulating in a wide pressure range, which resolves the long-standing debate on the possibility of this compound becoming a superconductor at experimentally reachable static pressures.

Pressure-induced superconductivity is one of the remarkable phenomena occurring in compressed matter and experimentally documented for many elements and compounds that are insulating at ambient pressure.[1,2] With the discovery of superconductivity in compressed lithium[3] and hydrogen-rich hydrides [e.g., group IV hydrides such as SiH$_4$ (Refs. 4 and 5) or theoretical predictions for SiH$_4$,[6] GeH$_4$,[7] and SnH$_4$ (Ref. 8)] and predicted unprecedentedly high T_c in metallic hydrogen,[9] the prospect of finding interesting superconducting materials among the compounds of light elements (especially hydrides) has become very exciting.

Lithium beryllium hydride, LiBeH$_3$, has long been considered a potential high-temperature superconductor due to the low mass of its constituent atoms and possibly strong electron-phonon coupling effects. Previous studies of its metallization and superconductivity have assumed the cubic perovskite structure.[10–12] Our recent *ab initio* total-energy calculations and global optimizations based on an evolutionary algorithm found that at ambient conditions LiBeH$_3$ crystallizes in a CaSiO$_3$-type structure with space group (SG) $P2_1/c$; this structure contains BeH$_4$ tetrahedra linked in chains (hereafter α-LiBeH$_3$).[13] At ambient conditions this material is an insulator [density-functional theory (DFT) band gap is 4.8 eV]. At sufficiently high pressures all materials are expected to be metallized, so the question is whether LiBeH$_3$ becomes a metal (and a superconductor) at static pressures that are experimentally achievable with today's experimental techniques (i.e., up to 300–350 GPa). In this paper, however, we report that LiBeH$_3$ remains an insulator up to the pressure of 530 GPa, the pressure at which it is predicted to break down into the mixture of LiH and BeH$_2$. The "stubborn" insulating behavior is explained by the electronic and atomic structure of this material and compares with elemental hydrogen, which has been predicted to become a metal only above 400 GPa.[14]

Our DFT calculations were performed using a plane-wave method within the generalized gradient approximation functional of Perdew and Wang,[15] as implemented in the Vienna

Ab initio Simulation Package (VASP).[16] The projector augmented wave (PAW) scheme[17] was used to describe the electron-ion interactions. An energy cutoff of 400 eV was used for the plane-wave basis sets, and the k-point spacing smaller than 0.03 Å^{-1} in the reciprocal space was used for all structures in order to minimize the error from the k-point meshes. The atomic positions, lattice parameters, and cell volume were fully optimized with an iterative matrix diagonalization scheme until the total energy is converged to 0.1 meV in the self-consistent loop and the force on each atom is less than 1 meV/Å.

To explore stable structures of LiBeH$_3$ under extreme conditions, an *ab initio* evolutionary algorithm (EA) as implemented in the USPEX (Universal Structure Predictor: Evolutionary Xtallography) code[18,19] was used. Currently, the EA simulations proved to be a very effective way to solve or predict crystal structure even in the absence of any experimental information, which is particularly suitable for exploring stable high-pressure structures. Various systems with known structures have been reproduced from evolutionary simulations and detected at a success rate close to 100%.[18,19] USPEX searches for the global minimum of *ab initio* (free) energy. All generated structures are locally optimized and compared on the basis of their optimized free energies (in practice, we do calculations at $T=0$ K, where the Gibbs free energy reduces to the enthalpy). Prior to local optimization we ensure that hard constraints (i.e., the minimal interatomic distances, the minimum value of a lattice parameter, and the minimum and maximum cell angles) are satisfied—otherwise, a candidate structure is rejected without local optimization. During simulations, no symmetry constraints are imposed, meaning that the resulting structures are dynamically stable without soft modes at the center of the Brillouin zone. The whole procedure of the EA structure search is sketched in brief as follows: (i) the first generation is produced randomly; (ii) the successive generations are obtained by applying heredity, mutation, and permutation operations, with probabilities of 60%, 20%, and 10%, respec-
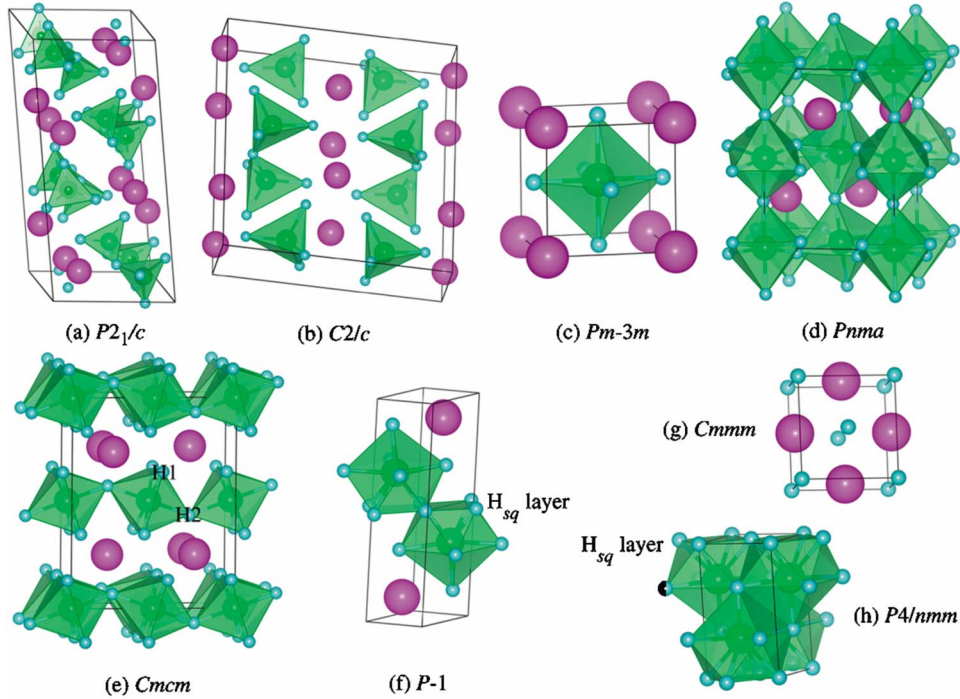
FIG. 1. (Color online) Crystal structures of $LiBeH_3$: (a) $P2_1/c$ ($CaSiO_3$-type), (b) C2/c ($MgSiO_3$-type) phase, (c) Pm-$3m$ (KMH_3-type) phase, (d) $Pnma$ ($GdFeO_3$-type) phase at 50 GPa, (e) $Cmcm$ ($CaIrO_3$-type) phase at 350 GPa, and (f) P-1 phase at 550 GPa; and its high-pressure dissociation products: (g) $Cmmm$ LiH and (h) $P4/nmm$ BeH_2. The polyhedra are BeH_4 in (a) $P2_1/c$ and (b) $C2/c$ phases, BeH_6 in (c) Pm-$3m$, (d) $Pnma$, and (e) $Cmcm$ phases, and BeH_9 in (f) P-1 and (h) $P4/nmm$ phases. The large and small spheres are Li and H, respectively. The nonequivalent H atoms in $Pnma$ and $Cmcm$ phases, and the squared-H atomic layer in P-1 for $LiBeH_3$ and P_4/nmm for BeH_2 are marked as "H1," "H2," and "H_{sq} layer." The structural parameters for the $P2_1/c$ and $C2/c$ phase can be found in our previous work (Ref. 13 in text).

tively, to the lowest energy of 60% of each generation; (iii) the simulation is stopped after the EA structure search reaches the given maximum generation numbers. More details about the EA simulations can be found in Refs. 18 and 19.

To investigate the structural stability and metallization of $LiBeH_3$ under extreme pressures, a complete high-pressure phase diagram must be established, which needs a reliable structure database to be built first. Following our previous work,[13] α-$LiBeH_3$ (SG: $P2_1/c$) and the monoclinic $MgSiO_3$-type (SG: $C2/c$) structures containing the BeH_4 tetrahedra linked in chains are considered as low-pressure candidates for $LiBeH_3$. In contrast, those competing structures containing the BeH_4 tetrahedra linked in rings are excluded in the current study, since we have found that they are always energetically unfavorable with increasing pressure.[13] To sample new stable structures under high pressures, variable-cell evolutionary simulations were performed for unit cells containing 10 and 20 atoms at pressures from 50 to 550 GPa in steps of 100 GPa. We also explored stable structures of LiH and BeH_2, using systems with 6 atoms/cell and 12 atoms/cell, respectively.

The cubic perovskite structure (SG: Pm-$3m$), studied in previous works, is identified by the EA simulations at 50 and 100 GPa for the unit cells with 5 atoms. For the EA simulations at 50 GPa for the system containing 20 atoms per unit cell, an orthorhombic perovskite structure (SG: $Pnma$) with $Z=4$ is found to be stable. Interestingly, across a wide pres-

sure range from 150 to 450 GPa, a base-centered orthorhombic phase (SG: $Cmcm$) with $Z=4$ is simultaneously detected to be favored in the EA simulations for the unit cells containing 10 and 20 atoms. The crystal structures and corresponding optimized structural parameters of the $Pnma$ phase at 50 GPa and the $Cmcm$ phase at 350 GPa are presented in Fig. 1 and Table I. The $Pnma$ phase shown in Fig. 1(d) is a three-dimensional framework structure build of corner-sharing BeH_6 octahedra. As shown in Fig. 1(e), the $Cmcm$ phase has a pronounced two-dimensional character and is composed of BeH_3 layers intercalated by Li ions. Be ions are in the sixfold-coordinated sites, forming the BeH_6 octahedral chains shared by H1-H1 edge and connected by H2 atoms that lie on octahedral apexes (see Fig. 1). Within BeH_3 layers Li ions are in the approximately eightfold-coordinated sites. The $Pnma$ and $Cmcm$ phases detected from the EA simulations are isostructural to the $GdFeO_3$-type perovskite[20] and $CaIrO_3$-type[21] structures, respectively. Especially, the $CaIrO_3$-type $Cmcm$ structure, as a prototype of high-pressure postperovskite phase of $MgSiO_3$, has received much attention lately since Oganov and Ono[22] and Murakami *et al.*[23] have found that the unusual physical properties of the high-pressure $Cmcm$ phase of $MgSiO_3$ explain many features of the Earth's lowermost mantle. The EA simulation at 550 GPa for the unit cell with 10 atoms yielded a new structure with space group P-1 presented in Fig. 1(f), in which each Be atom is coordinated to nine H atoms, forming a monocapped, square antiprism (BeH_9 polyhedron), and each Li atom is in

TABLE I. Optimized structural parameters of *Pnma* (GdFeO$_3$-type perovskite) phase at 50 GPa and *Cmcm* (CaIrO$_3$-type) phase at 350 GPa.

Symmetry	Lattice parameters (Å)		Internal atomic positions		
			x	y	z
Pnma	$a=3.957$	Li:	0.0558	0.2500	0.0124
$Z=4$	$b=5.498$	Be:	0.0000	0.0000	0.5000
	$c=3.820$	H1:	0.3044	0.0461	0.3078
		H2:	0.0226	0.7500	0.4075
Cmcm	$a=1.767$	Li:	0.0000	0.2447	0.2500
$Z=4$	$b=5.611$	Be:	0.0000	0.5000	0.0000
	$c=4.457$	H1:	0.0000	0.1503	0.5535
		H2:	0.0000	0.5674	0.2500

a sevenfold coordinated site, forming a square face monocapped, trigonal prism (LiH$_7$ polyhedron), respectively. This interesting and novel structure is less stable than the *Cmcm* structure up to 610 GPa. The theoretically optimized structural parameters of the *P*-1 phase are compiled in Table II.

The calculated enthalpy difference (ΔH) per formula unit (f.u.) with respect to α-LiBeH$_3$ as a function of pressure is displayed in Fig. 2. As presented in our previous work,[13] a structural transition from α-LiBeH$_3$ (SG: $P2_1/c$) to the $C2/c$ phase occurs at the pressure of 7 GPa. On further increase of pressure to 17 GPa, the *Pnma* perovskite phase becomes more stable than the $C2/c$ phase. The transition is strongly first-order and reconstructive, with a volume collapse of about 11%, and the coordination of Be ions changes from fourfold in low-pressure phases to sixfold in the *Pnma* phase. The *Cmcm* postperovskite phase is found to be energetically favorable in a wide pressure range from 140 up to 530 GPa. Above 530 GPa, as shown in Fig. 2, the *Cmcm*

phase decomposes into LiH and BeH$_2$ with space groups *Cmmm* and $P4/nmm$ [see Figs. 1(g) and 1(h)]. The relevant structural parameters are further presented in Table. II.

Present results, summarized in Fig. 2, enable a thorough understanding of structural transitions sequence for LiBeH$_3$. Adopting tetrahedral chain structures (pyroxenelike $P2_1/c$ and $C2/c$ phases) at low pressures, under pressure this material transforms to the GdFeO$_3$-type perovskite phase (space group *Pnma*), and then into the CaIrO$_3$ (*Cmcm*) postperovskite phase, and finally decomposes into LiH and BeH$_2$. This sequence is very similar to the one observed for many other ABX_3 compounds, for example MgSiO$_3$, the main component of the Earth's mantle. The transition from the perovskite *Pnma* to postperovskite *Cmcm* phases has been confirmed experimentally and theoretically not only in MgSiO$_3$,[22,23] but also in MgGeO$_3$,[24] NaMgF$_3$,[25] and many other compounds. EA simulations for MgSiO$_3$ presented by Oganov and Glass[18] have also detected the *Pnma* perovskite and *Cmcm*

TABLE II. Optimized structural parameters of the *P*-1 phase at 550 GPa for LiBeH$_3$, and the high-pressure dissociation products *Cmmm* and $P4/nmm$ phases at 530 GPa for LiH and BeH$_2$, respectively.

| Structure	Lattice parameters (Å, deg.)		Internal atomic positions		
			x	y	z
LiBeH$_3$ (*P*-1)	$a=1.751$	Li:	0.5472	0.2503	0.0942
$Z=2$	$b=1.848$	Be:	0.1658	0.7503	0.3327
	$c=5.613$	H1:	0.0564	0.7503	0.1127
	$\alpha=89.984$	H2:	0.6543	0.2504	0.3098
	$\beta=98.947$	H3:	0.2494	0.2501	0.4982
	$\gamma=90.003$				
LiH (*Cmmm*)	$a=2.182$	Li:	0.0000	0.5000	0.5000
$Z=2$	$b=2.228$	H:	0.0000	0.0000	0.0000
	$c=1.554$				
BeH$_2$ ($P4/nmm$)	$a=1.835$	Be:	0.5000	0.0000	0.2952
$Z=2$	$c=3.132$	H1:	0.0000	0.0000	0.0000
		H2:	0.0000	0.5000	0.3246
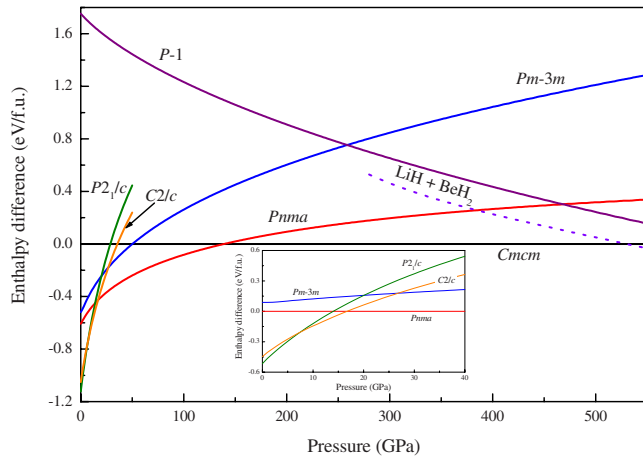
FIG. 2. (Color online) Calculated enthalpy differences (ΔH, in eV/f.u.), relative to the *Cmcm* (CaIrO$_3$-type) phase, as a function of pressure for various structures. For clarity the ΔH at low-pressure range below 40 GPa, with respect to the *Pnma* phase, is shown in the inset.
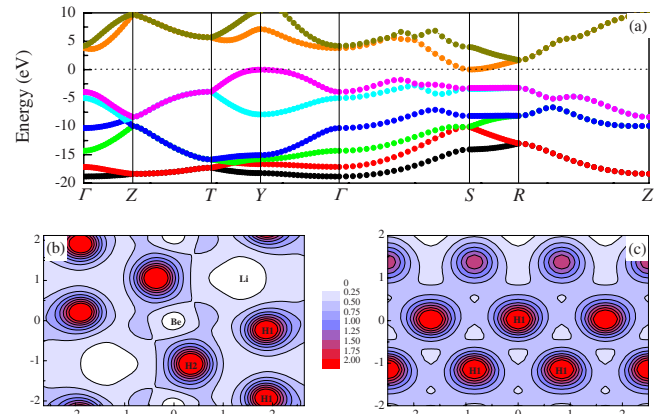

FIG. 3. (Color online) Electronic structure of the *Cmcm* phase at 530 GPa: (a) band structure; [(b) and (c)] difference charge-density distribution for the slices across the H1-Be-H2 and H1-H1-H1 atomic planes (see Fig. 1), respectively. The units of charge density are in $e/\text{Å}^3$ and distances in Å.

postperovskite phases. Based on first-principles quasiharmonic free-energy calculations, Umemoto *et al.*[26] have further deduced that the CaIrO$_3$-type structure seems to be the ultimate high-pressure structure of MgSiO$_3$ before it dissociates into MgO and SiO$_2$. It is not too surprising that a similar high-pressure behavior is exhibited by LiBeH$_3$, considering the fact stressed in our previous work[13] that the structural relation between LiBeH$_3$ and silicates is very close.

We next turn to discuss the possibility of the metallization in LiBeH$_3$. Metallization of any compound should occur by band overlap.[1] The calculated electronic densities of states (DOS) within DFT show that the distorted-perovskite *Pnma* phase is an insulator with a pronounced band gap even at the pressure of 500 GPa. This is in contrast with the undistorted perovskite *Pm*3*m* structure, which becomes metallic at 160 GPa,[11] but is substantially less stable. However, above 140 GPa and all the way up to the decomposition pressure (530 GPa), the CaIrO$_3$-type *Cmcm* structure is the most stable one (see Fig. 2). Figure 3 demonstrates the electronic band structure and deformation charge-density distribution (i.e., the difference between the actual charge density and the sum of noninteracting atomic densities) for the *Cmcm* structure at 530 GPa. As Fig. 3(a) shows, a tiny indirect energy gap of about 0.02 eV still exists between *Y* and *S* points in the Brillouin zone. Based on the fact that the band gap from DFT calculations are normally underestimated compared to the experimental value, at 530 GPa the real band gap of the *Cmcm* phase should be larger and this phase should be a semiconductor at this pressure. The *P*-1 phase becomes metallic at a much lower pressure of 280 GPa, which is due to close H-H distances (1.38 Å) within the almost square layer of hydrogen atoms, as shown in Fig. 1(c). However, this remarkable structure is never thermodynamically stable. To compare with the previous work made on the assumed *Pm*-3*m* cubic perovskite phase,[10–12] we have also investigated the metallization of the *Pm*-3*m* phase. As the lattice constant is reduced to $a=2.46$ Å as presented in the work of Gupta and Percheron-Guegan,[11] the *Pm*-3*m* phase is indeed

metallic with a small DOS at Fermi level. This lattice parameter corresponds to the pressure of 164 GPa, where the stable phase of LiBeH$_3$ has the insulating *Cmcm* structure. Moreover, our static enthalpy calculations have shown that the *Pm*-3*m* phase is not energetically favorable in the whole pressure range considered here (see Fig. 2). On the whole, according to our calculations, we have found that LiBeH$_3$ still remain nonmetallic even pressure up to 530 GPa, which contradicts previous conclusion drawn on the assumption of the cubic perovskite *Pm*-3*m* phase.[10–12]

However, it is noteworthy that at 530 GPa and even lower pressure the dissociation products of LiBeH$_3$, LiH, and BeH$_2$, are indeed metallic. Especially, at 530 GPa the high DOS at Fermi level of the *P*4/*nmm* BeH$_2$ indicates that BeH$_2$ is a good metal. This is mainly related to the significant overlap of the electron densities of the H atoms due to short H-H contacts below 1.30 Å in a squared-H atomic layer for the *P*4/*nmm* BeH$_2$ [see Fig. 1(h)], very similar to the atomic arrangement of Be and H ions in the metastable *P*-1 form of LiBeH$_3$. Under pressure, BeH$_2$ might become an interesting superconductor, and this warrants a separate study.

Why is LiBeH$_3$ so hard to be metallized? The band gap is formed by 1s-levels of hydrogen [highest occupied molecular orbital (HOMO)] and 2s-levels of lithium and beryllium atoms [lowest unoccupied molecular orbital (LUMO)]. Among several possibilities for closing the band gap, the most natural one is to broaden the hydrogen 1s band by bringing the H atoms closer together. One rough criterion of metallization of hydrides could be the formation of extended H substructures with H-H distances comparable to twice the 1s orbital radius of the hydrogen atom—i.e., 1.06 Å, and this is indeed a short distance (based on the results of this work, even the distance of 1.4 Å seems sufficient, but this is still a short distance). Although the bonding in BeH$_2$ is mixed ionic covalent, due to the presence of a low-electronegativity atom, lithium, LiBeH$_3$ is a predominantly ionic compound.[13] Establishing close H-H contacts in an ionic hydride is particularly difficult due to the Coulomb

repulsion between the H$^-$ ions, and also due to the repulsion of their filled electronic shells. For more covalent hydrides these difficulties are greatly reduced, and metallization with interesting superconducting properties was predicted in SiH$_4$,[6] GeH$_4$,[7] and SnH$_4$ (Ref. [8]) at experimentally reachable pressures of $\sim$100–200 GPa. In this work, we predicted metallization of BeH$_2$ to occur at 270 GPa, and it can indeed be an interesting superconductor. All of these metallic phases have H-H contacts of 1.4 Å or shorter. Ionicity of a hydride does not only determine the ease of its metallization, but could also be related to the T_c value. The more ionic a hydride, the higher is electron density around the H atom. While contributing to the H-H repulsion, once the H atoms are placed close together, this factor can be expected to lead to increased DOS values at the Fermi level and higher T_c values. This is why BeH$_2$, which does become metallic at experimentally reachable pressures, can have high T_c values and requires further study. Ionicity of LiBeH$_3$ is also closely linked with the structural transition sequence, which mirrors that of many ionic ABX_3 compounds[22–26] and contains a gigantic stability field of the *Cmcm* postperovskite phase.

In conclusion, we have investigated the structural stability and possibility of metallization of LiBeH$_3$ under extreme pressures using *ab initio* total-energy calculations and evolutionary structure searches. The low-pressure phase containing chains of BeH$_4$ tetrahedra undergoes a structural transition to the GdFeO$_3$-type perovskite structure (*Pnma*) with the BeH$_6$ octahedra at 17 GPa, then the *Pnma* phase transforms into a CaIrO$_3$-type postperovskite structure (*Cmcm*) at 140 GPa, and finally the compound decomposes into LiH (*Cmmm*) and BeH$_2$ (*P4/nmm*) at 530 GPa. The high-pressure behavior is entirely similar to that of other ABX_3 analogs such as MgSiO$_3$. Our band-structure calculations suggest that at the level of density-functional theory the *Cmcm* phase of LiBeH$_3$ remains nonmetallic even at the decomposition pressure of 530 GPa, where it has a tiny indirect band gap of about 0.02 eV.

*Corresponding author; chaohao.hu@guet.edu.cn

[1] J. B. Neaton and N. W. Ashcroft, Nature (London) **400**, 141 (1999).

[2] N. W. Ashcroft, Phys. Rev. Lett. **92**, 187002 (2004).

[3] K. Shimizu, H. Ishikawa, D. Takao, T. Yagi, and K. Amaya, Nature (London) **419**, 597 (2002).

[4] X. J. Chen, V. V. Struzhkin, Y. Song, A. F. Goncharov, M. Ahart, Z. X. Liu, H. K. Mao, and R. J. Hemley, Proc. Natl. Acad. Sci. U.S.A. **105**, 20 (2008).

[5] M. I. Eremets, I. A. Trojan, S. A. Medvedev, J. S. Tse, and Y. Yao, Science **319**, 1506 (2008).

[6] M. Martínez-Canales, A. R. Oganov, Y. M. Ma, Y. Yan, O. Lyakhov, and A. Bergara, Phys. Rev. Lett. **102**, 087005 (2009).

[7] G. Gao, A. R. Oganov, A. Bergara, M. Martinez-Canales, T. Cui, T. Iitaka, Y. Ma, and G. Zou, Phys. Rev. Lett. **101**, 107002 (2008).

[8] J. S. Tse, Y. Yao, and K. Tanaka, Phys. Rev. Lett. **98**, 117004 (2007).

[9] P. Cudazzo, G. Profeta, A. Sanna, A. Floris, A. Continenza, S. Massidda, and E. K. U. Gross, Phys. Rev. Lett. **100**, 257001 (2008).

[10] A. W. Overhauser, Phys. Rev. B **35**, 411 (1987).

[11] M. Gupta and A. Percheron-Guegan, J. Phys. F **17**, L201 (1987).

[12] R. Yu and P. K. Lam, Phys. Rev. B **38**, 3576 (1988).

[13] C. H. Hu, A. R. Oganov, Y. M. Wang, H. Y. Zhou, A. Lyakhov, and J. Hafner, J. Chem. Phys. **129**, 234105 (2008).

[14] K. A. Johnson and N. W. Ashcroft, Nature (London) **403**, 632 (2000).

[15] J. P. Perdew and Y. Wang, Phys. Rev. B **45**, 13244 (1992).

[16] G. Kresse and J. Furthmüller, Comput. Mater. Sci. **6**, 15 (1996).

[17] G. Kresse and D. Joubert, Phys. Rev. B **59**, 1758 (1999).

[18] A. R. Oganov and C. W. Glass, J. Chem. Phys. **124**, 244704 (2006).

[19] C. W. Glass, A. R. Oganov, and N. Hansen, Comput. Phys. Commun. **175**, 713 (2006).

[20] S. Geller and E. A. Wood, Acta Crystallogr. **9**, 563 (1956).

[21] C. L. McDaniel and S. J. Schneider, J. Solid State Chem. **4**, 275 (1972).

[22] A. R. Oganov and S. Ono, Nature (London) **430**, 445 (2004).

[23] M. Murakami, K. Hirose, K. Kawamura, N. Sata, and Y. Ohishi, Science **304**, 855 (2004).

[24] K. Hirose, K. Kawamura, Y. Ohishi, S. Tateno, and N. Sata, Am. Mineral. **90**, 262 (2005).

[25] H.-Z. Liu, J. Chen, J. Hu, C. D. Martin, D. J. Weidner, D. Hausermann, and H. K. Mao, Geophys. Res. Lett. **32**, L04304 (2005).

[26] K. Umemoto, R. M. Wentzcovitch, and P. B. Allen, Science **311**, 983 (2006).